Research Article

Nonlinear Quantum-Inspired Weighting Structuring Element for Bearing Impulse Response Signal Processing

Guoquan Ren ⬥,[1] Yanlong Chen,[2] Chengzhu Li,[2] and Ziyang Cheng ⬥[1]

[1]*Army Engineering University, Shijiazhuang, China*
[2]*Army Special Operations Academy, Guilin, China*

Correspondence should be addressed to Guoquan Ren; rrrgggqqq@163.com

In order to solve the disadvantage of conventional structuring element (CSE) where amplitude does not change in accordance with the analyzed signal, the quantum theory is combined and a nonlinear quantum-inspired weighting structuring element (NQWSE) is proposed. The NQWSE which is utilized to extract the bearing impulse response signal can adjust its amplitude according to the mechanical signal. Firstly, after constructing the multiple quantum bits system for signals, the mapping method which is employed to map the quantum space to the real space is presented and the parameters of the mapping method are set. The nonlinear amplitude probability is calculated based on the stochastic characteristics of the bearing signals, while the dynamic amplitude is calculated based on the local feature of the bearing signals in a subwindow. Then the mathematical formula of NQWSE is derived by incorporating the mathematical expectation into the quantum theory and the mapping method. Finally, the NQWSE is applied to extract the fault information of a failure bearing. The results reveal that NQWSE can extract the bearing impulse response signals exactly.

1. Introduction

When the bearing of mechanical equipment fails, collisions occur between the damaged component and the other components. Each collision gives an impulse force to the bearing system and the impact is the source of a mechanical vibration signal. In the vibration signal collected from a failure bearing, the impact is represented as an impulse response signal. The impulse response signal which has remarkable local feature will be produced in the bearing operation during time after time. On the contrary, the working condition of mechanical equipment is relatively complex and the working condition is not stable. This actuality implies randomness which will lead to stochastic characteristics hidden in bearing sampling signal.

The impulse factor can reflect the shock degree of impulse response signal, and it can be employed to measure the local feature of a bearing signal [1–3]. Rodríguez et al. [1] used the impulse factor to perform the classification of bearing failure. Zhang et al. [2] proposed a new fault diagnosis method based on multiple features which included impulse factor of the roller bearing signal. Pandya et al. [3] also utilized the impulse factor to describe the feature of the bearing signal, and the fault diagnosis of ball bearing was reliable. In our research, the impulse factor is also adopted to depict the local feature of the impulse response signal.

The empirical mode decomposition (EMD) [4] and wavelet technique [5] are among the most popular approaches to process signals in the area of bearing fault detection. The EMD shows outstanding performance in processing nonlinear and nonstationary signals. However, EMD has several problems such as mode mixing, end effects, interpolation problems, stopping criterion [6], and so on. Owing to the adaptive and multiresolution capability, the wavelet technique has become a powerful mathematical tool for bearing diagnosis. However, there still exist some challenges in using wavelets because of the fact that the more similar the signal is to the wavelet function, the better the defect related features will be extracted [7]. Mathematical morphological filter (MMF) [8] has become an efficient tool

for signal processing in recent years and provides an alternative mean to extract impulsive signals purely based on time-domain analysis. Therefore, the application of MMF to locate bearing faults in recent years has attracted a lot of attention [9, 10]. Li and Xiao [9] proposed a supervised pattern classification algorithm on the basis of one-dimensional adaptive rank order MMF and diagnosis for real faulted rolling bearings indicated its efficiency. Li et al. [10] presented weighted multiscale morphological gradient filter for rolling element bearing fault detection. However, the studies [9, 10] employ the conventional structuring element (CSE) to perform the morphological analysis, which means the amplitude of the structuring element (SE) will not vary while the signal varies according to time and working condition. In other words, CSE inevitably ignores the local feature and stochastic characteristics of the bearing vibration signal, which severely limits the filtering effects. In order to enhance the analyzing capability of MMF for faulted bearing vibration signal, it is necessary to take local feature and stochastic characteristics into consideration to dynamically adjust the amplitude of SE.

The erosion operator of MMF has some capability to extract the impulse response signal and the erosion operator is one of the basic operators which are the basis to form other more complex morphological operators [8]. In order to extend the theoretical value and application value of the research contents, this paper focuses on studying the SE used for the erosion operator.

In recent years, the quantum theory has been developed rapidly in the field of data optimization [11, 12], quick search [13, 14], signal transmission [15, 16], image processing [17, 18], etc., and comes into use with many projects, which reveals that this theory has a huge potential for research. In this article, combining the quantum knowledge with the local feature and stochastic characteristics of signal, the nonlinear quantum-inspired weighting structuring element (NQWSE) is presented. The amplitude of NQWSE can adjust dynamically as the signal varies, and thus, it improves extraction ability for the impulse response signal. Firstly, the feasibility of multiple quantum bits system to represent states of SE is discussed. Then a method of mapping the quantum-inspired-state structuring element (QSSE) to quantum-inspired mapping structuring element (QMSE) is proposed. The impulse factor which depicts the local feature of the impulse response signal is used to compute the amplitude of QMSE in real space and the signal is normalized to compute the amplitude probability of each QMSE. Next, incorporating quantum theory into mathematic expectation, all the QMSEs are compounded as one NQWSE. The NQWSE is applied to the erosion operator of MMF and the detection of bearing fault is performed. The results verify the extraction ability of NQWSE for bearing impulse response signal.

2. Research Object

2.1. Research Object of MMF.
The erosion operator of MMF has some ability to extract failure information. Furthermore, it is the basis to form other morphological operators and the

premise to construct more complex filters. The research on the erosion operator has a much broader sense, so this paper will focus on discussing about designing SE according to the erosion operator.

Since the SE is a vector, for the convenience of elaboration, the signal is also treated as a vector. Let us assume that the input signal is $\mathbf{s}(k)$ $(k = 1, 2, \ldots, l)$ and the SE is $\mathbf{g}(j)$ $(j = 1, 2, \ldots, n)$ while $l \gg n$.

The erosion operator is defined as

$$(\mathbf{s}\Theta\mathbf{g})(k) = \min\{\mathbf{s}(k + j - 1) - \mathbf{g}(j) \mid j = 1, 2, \ldots, n\}. \quad (1)$$

It is observed in equation (1) that the main purpose of erosion is to set to a much lower extent the lower value of the signal. However, when the fault occurs, the impulse response signal generates and the sampled signal will suddenly increase. So there exists a contradiction between the erosion operator and the failure information extraction. In order to extract exact failure information, the signal is inverted here (namely, multiplying the vibration signal by −1). The time at which the fault occurs can be detected finding the time at which the signal decreases suddenly. So, after the erosion, the value corresponding to impulse response signal becomes much lower, which means the information of the failure will be highlighted. After inverting, $\mathbf{s}(k)$ turns into $\mathbf{rs}(k)$:

$$\mathbf{rs}(k) = -\mathbf{s}(k). \quad (2)$$

2.2. Extraction Object of SE.
As different SEs used for erosion operator can extract different information in bearing vibration signals, it is firstly necessary to confirm the extraction object of SE. In this paper, the sampled signal is the online monitoring signal which is used to acquire the failure information of the bearing. In order to obtain the failure information exactly and ascertain the failure position, it is necessary to extract the impulse response signal. Therefore, the SE is mainly used to extract the impulse response signal in the vibration signal.

3. Feasibility Analysis of Introducing Quantum Theory into SE Design

3.1. Multiple Quantum Bits System.
The quantum bit is the basic unit to form the multiple quantum bits system. One state of a quantum bit is a linear combination of two states $|0\rangle$ and $|1\rangle$. The mathematical expression of a quantum bit is formulated as [19–21]

$$|\Psi\rangle = \alpha|0\rangle + \beta|1\rangle, \quad (3)$$

where α and β are the probability amplitudes of the corresponding states $|0\rangle$ and $|1\rangle$ and $|\alpha|^2$ and $|\beta|^2$ are the appearance probability that the quantum bit will be in the $|0\rangle$ state and $|1\rangle$ state, respectively.

α and β are the complex numbers, and the following normalization condition is always satisfied:

$$|\alpha|^2 + |\beta|^2 = 1. \quad (4)$$

To extend the quantum bit on the basis of equation (3), assuming that n quantum bits make up a quantum system, this multiple quantum bits system can be expressed as [22]

$$
\begin{aligned}
|\mathbf{I}\rangle &= \left(w_0^1 \times w_0^2 \times \cdots \times w_0^j \times \cdots \times w_0^n\right)|00\cdots 0\rangle \\
&\quad + \left(w_0^1 \times w_0^2 \times \cdots \times w_0^j \times \cdots \times w_1^n\right)|00\cdots 1\rangle + \cdots \\
&\quad + \left(w_1^1 \times w_1^2 \times \cdots \times w_1^j \times \cdots \times w_1^n\right)|11\cdots 1\rangle \\
&= \sum_{i=0}^{2^n-1} \mathbf{W}_i |\mathbf{i}_b\rangle,
\end{aligned}
$$

(5)

where $j\,(j = 1, 2, \ldots, n)$ denotes the jth quantum bit of the n quantum bits system. $|\mathbf{i}_b\rangle$ denotes the ground states of the n quantum bits system. $\mathbf{i}_b$ is the binary expression corresponding to the decimal number $\mathbf{i}$, $|\mathbf{i}_b\rangle \in \{|00\ldots 0\rangle, \ldots, |11\ldots 1\rangle\}$. It can be observed that in equation (5), w_1^j denotes the probability amplitude corresponding to state $|1\rangle$ of the jth quantum bit $|\mathbf{i}_b\rangle\,(j)$ and w_0^j denotes the probability amplitude corresponding to state $|0\rangle$ of the jth quantum bit $|\mathbf{i}_b\rangle\,(j)$. $\mathbf{W}_i$ is the probability amplitude of the ground state $|\mathbf{i}_b\rangle$. $\mathbf{W}_i^2$ give the appearance probability that the ground state will be in the $|\mathbf{i}_b\rangle$ state, and it satisfies the normalizing condition:

$$
\sum_{i=0}^{2^n-1} |\mathbf{W}_i|^2 = 1.
$$

(6)

The multiple quantum bits system can be understood as the superposition of multiple ground states. Compared with the ground state of single quantum bit, each ground state of multiple quantum bits system is more complex and contains richer information. The multiple quantum bits system contains multiple ground states $|\mathbf{i}_b\rangle \in \{|00\cdots 0\rangle, \ldots, |11\cdots 1\rangle\}$. If different ground states corresponds to different SEs, the binary ground states $|\mathbf{i}_b\rangle$ of multiple quantum bits system in quantum space can be mapped to corresponding decimal states in real space via an appropriate mapping method. And then the NQWSE can be constructed.

3.2. Feasibility Analysis. The bearing vibration signal possesses two characteristics of nonlinearity and instability. The amplitude of CSE keeps constant when it is used in MMF, which means that the CSE ignores the nonlinearity and instability of signal. Adopting the CSE to directly analyze such signal has limits in extracting information. Hence, in order to achieve a greater adaptive capability to signal and to enhance the extraction of the related information, a SE which can adjust its amplitude according to the signal can greatly improve the detection of bearing failures. The multiple quantum bits system contains multiple ground states; for example, one n quantum bits system contains $2n$ ground states. If one ground state $|\mathbf{i}_b\rangle$ corresponds to one SE, then one n quantum bits system can represent $2n$ SEs. Considering both local feature and stochastic characteristics comprehensively, by controlling the weighting of different SEs, the different SEs can be merged together. The amplitude of the acquired SE in the end varies as the amplitude of the

signal varies, which overcomes the disadvantages of CSE. Then the processing ability of nonlinear and nonstable signals is improved while benefitting from this merit. Therefore, the quantum theory is introduced to the SE designing.

The more quantum bits the multiple quantum bits system possesses, the more the ground states it contains. The more the SEs to be used for signal analysis, the more the space MMF can be operated in. However, as n increases, the amount of calculation increases exponentially. When $n = 5$, there are 2^5 SEs. When $n = 46$, there are up to 2^{46} SEs. Considering both computation speed and analysis ability of signal, $n = 5$ in this paper.

The sampling vibration signal of one bearing is made of a real number. When the MMF processes a real number, an SE of the real number is asked for. Hence, the binary expression as equation (5) in quantum space is unavailable to vibration signal analysis. Aiming at this problem, the specific mapping method, which maps the binary ground states $|\mathbf{i}_b\rangle$ from the quantum space to the decimal form in real space, will be presented in the next section.

4. Mapping Method from the Quantum Space to the Real Space

4.1. Mapping Method. On the basis of quantum theory, after quantum measurement, the quantum system $|\mathbf{I}\rangle$ will become a certain ground state which is represented as $|\mathbf{i}_b\rangle$. $|\mathbf{i}_b\rangle$ denotes the ground state of SE in quantum space, for ease to understand the mapping method below, the binary $|\mathbf{i}_b\rangle$ is named the quantum-inspired state structuring element (QSSE). If the QSSE is mapped to the real space, it becomes a decimal SE, which is named quantum-inspired mapping structuring element (QMSE).

According to the erosion formula in equation (1), the length of SE (decimal) equals n. Let the length of the binary ground state $|\mathbf{i}_b\rangle$ equals the length of decimal SE. The $|\mathbf{i}_b\rangle\,(j)$ is used to denote the jth bit of the binary ground state $|\mathbf{i}_b\rangle$, so the corresponding bit of the decimal vectorial SE is denoted as $\mathbf{g}(j)$. If the state $|0\rangle$ of binary $|\mathbf{i}_b\rangle\,(j)$ represents one state of decimal $\mathbf{g}(j)$ and the state $|1\rangle$ of binary $|\mathbf{i}_b\rangle\,(j)$ represents the other state of decimal $\mathbf{g}(j)$, the specific mapping method is explained in detail as follows:

(1) The probability amplitude of state $|1\rangle$ in $|\mathbf{i}_b\rangle\,(j)$ is w_1^j. After measuring the quantum system, the QSSE is obtained. When the QSSE is mapped as QMSE, the corresponding amplitude of bit $\mathbf{g}(j)$ equals $\mathbf{r}_j$, where $\mathbf{r}_j$ is the quantitative description of local feature.

(2) The probability amplitude of state $|0\rangle$ in $|\mathbf{i}_b\rangle\,(j)$ is w_0^j. After measuring the quantum system, the QSSE is obtained. When the QSSE is mapped as QMSE, the corresponding amplitude of bit $\mathbf{g}(j)$ equals 0.

The amplitude $\mathbf{r}_j$ and probability amplitude are the two key parameters in the mapping method, and they will be discussed in the next two sections. Each QMSE achieved by the mapping method above is a certain SE, which can be applied to MMF directly. The mapping relation between QSSE and QMSE is illustrated in Figure 1.
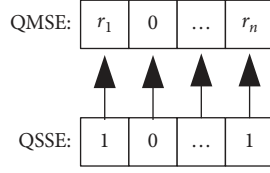
QMSE: | r_1 | 0 | ... | r_n |

QSSE: | 1 | 0 | ... | 1 |

FIGURE 1: Mapping relation between QSSE and QMSE.

4.2. Amplitude of QMSE Based on Local Feature. In the previous section, it has been shown that the amplitude $\mathbf{r}_j$ severely affects the analyzing capacity. Considering both the erosion operator and the mapping method, $\mathbf{r}_j$ should help lowering the value of $\mathbf{z}(k)$ more notably when $\mathbf{z}(k)$ is less, which can outstand the impulse response signal for extracting failure information. The impulse factor of the sampling signal is adopted as the indicator to reflect the shock degree of the sampling signal:

$$\mathbf{r}(k) = \frac{\max(\mathbf{sw}(k))}{|\text{mean}(\mathbf{sw}(k))|}. \tag{7}$$

To highlight the local feature of the failure signal as far as possible, $\mathbf{sw}$ is a signal segment which is a subwindow center at the sampling point. The width of the subwindow is 5 and $\mathbf{sw}(k) = [\mathbf{s}(k-2), \mathbf{s}(k-1), \mathbf{s}(k), \mathbf{s}(k+1), \mathbf{s}(k+2)]$.

While the erosion operator is processing the k-th sampling point, the data segment operated by erosion is $[\mathbf{rs}(k), \mathbf{rs}(k+1), \ldots, \mathbf{rs}(k+j-1), \ldots, \mathbf{rs}(k+n-1)]$. After mapping QSSE to QMSE, $\mathbf{r}_j$ is represented as

$$\mathbf{r}_j = r(k+j-1), \quad j = 1, 2, \ldots, n. \tag{8}$$

It is noted that $r_1 \neq r_2 \neq \cdots \neq r_n$ since the signal is stochastic. When $|\mathbf{i}_b\rangle = |11\cdots1\rangle$, $\mathbf{g} = [r_1, r_2, \ldots, r_n]$, QMSE is determined by local impulse factor thoroughly. Considering both the erosion operator and inverted signal $\mathbf{rs}(k)$ in equation (2), the quantitative description $\mathbf{r}_j$ for local feature guarantees that the sampling point corresponding to impulse response signal will be highlighted when the erosion is operated, which means the sampling point of the inverted signal containing failure information will become less. These advantages are very useful for extracting failure information.

4.3. Nonlinear Amplitude Probability Based on Stochastic Characteristics. After mapping, different QSSEs become corresponding QMSEs. However, different QMSEs have different appearance probability. The probability amplitude (w_0^j, w_1^j) has great impact on the appearance probability of QMSE. Since different QMSEs have different influences on processing the same signal, the setting of the probability amplitude must be reasonable. The issue is the stochastic characteristics of the signal when the quantum probability is set.

For further restriction, (w_0^j, w_1^j) is required to meet two conditions:

$$0 \leq w_0^j \leq 1, \tag{9}$$

$$0 \leq w_1^j \leq 1. \tag{10}$$

According to equations (1), (2), (7), and (8), it is known that applying the erosion operators to $\mathbf{s}(k)$ for extracting the impulse response signal is applying to $\mathbf{rs}(k)$ in nature. To meet the two conditions in equations (9) and (10), the normalized vibration signal is incorporated into the trigonometric function to act as the probability amplitude of the ground state [22, 23]. Equation (11) is employed to normalize the inverted signal $\mathbf{rs}(k)$ [24]:

$$\mathbf{z}(k) = \frac{\mathbf{rs}(k) - \min(\mathbf{rs}(k))}{\max(\mathbf{rs}(k)) - \min(\mathbf{rs}(k))}. \tag{11}$$

For the normalized signal, the time corresponding to impulse response signal has a lower value, while the time not corresponding to impulse response signal has a higher value. When the erosion operator deals with the k-th sampling point, the data segment operated with erosion is $[\mathbf{rs}(k), \mathbf{rs}(k+1), \ldots, \mathbf{rs}(k+j-1), \ldots, \mathbf{rs}(k+n-1)]$ and its corresponding inverted normalized value is $[\mathbf{z}(k), \mathbf{z}(k+1), \ldots, \mathbf{z}(k+j-1)], \ldots, \mathbf{z}(k+n-1)]$ $(j = 1, 2, \ldots, n; k = 1, 2, \ldots, l)$.

Considering the mapping method, the larger the inverted normalized signal $z(k)$ is, the lower is the probability that there exists an impulse response signal. In this situation, we try not to reduce the value of $z(k)$; that is to say, we try to keep the value which is not corresponding to impulse response signal as invariable as possible. When $|\mathbf{i}_b\rangle(j) = |0\rangle$, $\mathbf{g}(j) = 0$ exists. For this reason, the probability amplitude of the ground state $|0\rangle$ in $|\mathbf{i}_b\rangle(j)$ is represented as

$$w_0^j = \sin(\mathbf{z}(k+j-1)). \tag{12}$$

To satisfy the normalizing condition of the quantum system, the cosine function incorporating with the normalized signal is adopted to represent the probability amplitude of the ground state $|1\rangle$ in $|\mathbf{i}_b\rangle(j)$:

$$w_1^j = \cos(\mathbf{z}(k+j-1)). \tag{13}$$

The amplitude probability of the states $|0\rangle$ and $|1\rangle$ is represented as the sinusoidal function and the cosine function. Simultaneously the appearance probability of the states $|0\rangle$ and $|1\rangle$ is the square of the two functions. The reason why the NQWSE is named "nonlinear" is that both the amplitude probability and the appearance probability are nonlinear.

By incorporating the normalized signal into trigonometric function, the probability amplitude of $|\mathbf{i}_b\rangle(j)$ is generated, which is equivalent to taking the stochastic characteristics of signal into account for computing probability amplitude. This eliminates the disadvantage of manually setting probability amplitude. After mapping, at one sampling point, the larger the $\mathbf{z}(k)$ is, the lower is the possibility that a failure may occur, and the lower is the possibility that the impulse response signal may exist. Moreover, the larger probability $\mathbf{g}(j) = 0$ has, the higher is the possibility that erosion operator do not change the value. The less the $\mathbf{z}(k)$ is, the more possibly the failure may occur. And the more possibly the failure may occur. And the more possibly the impulse response signal may exist. Moreover, the larger probability $\mathbf{g}(j) = \mathbf{r}_j$ has, thus the more possibly erosion operator changes the value. Therefore, setting

probability amplitude using equations (12) and (13) can ensure that the SE changes as less as possible the values not containing failure information as less as possible. At the same time, the setting approach can give prominence as more as possible to the values containing failure information, for the purpose of extracting failure information.

Above all, the formation process of NQWSE is illustrated in Figure 2.

5. Generation of NQWSE and Its Property

5.1. Formula of NQWSE. We continue the analysis of equation (5). After quantum measurement, equation (5) will collapse as a certain QSSE. Its expression is denoted as **qsse**:

$$\mathbf{qsse} \in \{|00\cdots0\rangle, |00\cdots1\rangle, \ldots, |11\cdots1\rangle\}. \quad (14)$$

The probability amplitude of $\mathbf{W}_i$ is as follows:

$$\mathbf{W}_i \in \left\{w_0^1 \times w_0^2 \times \cdots \times w_0^n, \ldots, w_1^1 \times w_1^2 \times \cdots \times w_1^n\right\}. \quad (15)$$

In physical world, the quantum system can only exhibit one determinate state. The erosion for multiple quantum bits system is erosion for QSSE, in the following formula:

$$\mathbf{s}\Theta|\mathbf{I}\rangle = \mathbf{s}\Theta\mathbf{qsse}. \quad (16)$$

Integrating with (15), the appearance probability of $\mathbf{s}\Theta\mathbf{qsse}$ in quantum space is

$$p(\mathbf{s}\Theta\mathbf{qsse}) = \mathbf{W}_i^2. \quad (17)$$

Based on quantum theory, the mathematical expectation of erosion for multiple quantum bits system is

$$E(\mathbf{s}\Theta|\mathbf{I}\rangle) = \sum_{i=0}^{2^n-1} W_i^2 \times (\mathbf{s}\Theta\mathbf{qsse}). \quad (18)$$

Incorporating with the mapping method, after mapping equation (14) to real space, the QSSE becomes QMSE and its mathematical expression is

$$\mathbf{qmse} \in \left\{[0, 0, \ldots, 0], [0, 0, \ldots, r_n], \ldots, [r_1, r_2, \ldots, r_n]\right\}. \quad (19)$$

Since one QSSE is mapped as one specific QMSE, the probability of generating QMSE equals that of generating QSSE. The erosion probability of them is the same:

$$p(\mathbf{s}\Theta\mathbf{qsse}) = p(\mathbf{s}\Theta\mathbf{qwse}) = W_i^2. \quad (20)$$

Combining equations (18) and (19) with equation (20), mathematical expectation is employed to merge the information of all the QMSEs. The NQWSE is the composition of QMSEs, and it is represented as

$$\mathbf{qwse} = W_0^2[0, 0, \ldots, 0] + W_1^2[0, 0, \ldots, r_n] + \cdots$$
$$+ W_{2^n-1}^2[r_1, r_2, \ldots, r_n]. \quad (21)$$

Signal segment for erosion to process is $[\mathbf{rs}(k), \mathbf{rs}(k+1), \ldots, \mathbf{rs}(k+j-1), \ldots, \mathbf{rs}(k+n-1)]$, which corresponding inverted normalized value is $[\mathbf{z}(k), \mathbf{z}(k+1), \ldots, \mathbf{z}(k+j-1), \ldots, \mathbf{z}(k+n-1)]$. As for probability amplitude W_i, if there is no impulse response
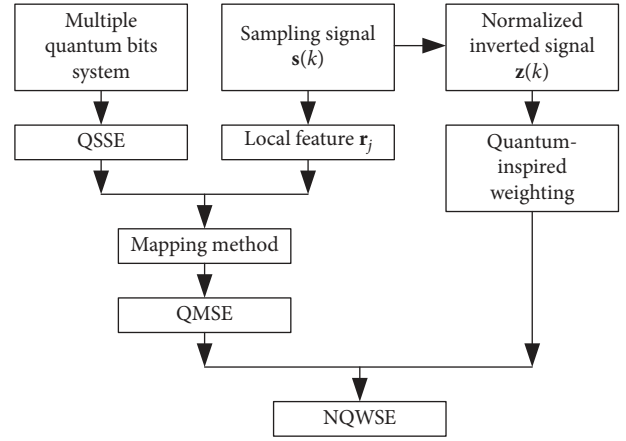

FIGURE 2: Generating process of the NQWSE.

signal in this segment, the value of W_0^2 is larger, the weighting of $[0, 0, 0, \ldots, 0]$ is larger. If the segment is totally impulse response signal, the value of $W_{2^n-1}^2$ is larger, the weighting of $[r_1, r_2, \ldots, r_n]$ is larger. Likewise, whenever the impulse response signal exists, the QMSE corresponding to the structure has larger weighting in NQWSE. For example, if $\mathbf{z}(k+1)$ is related to impulse response signal and the others are not, $[0, r_2, 0, \ldots, 0]$ will have a larger weighting. Above all, the NQWSE can adjust adaptively according to signal variation.

It is observed in equation (21) that different QMSEs have different weightings in the NQWSE; therefore the corresponding weightings of different QMSEs can be regarded as quantum-inspired weighting. It can be seen that, in the computation process, the quantum-inspired weighting W_i^2 and $\mathbf{r}_j$ of each QMSE are the key parameters which make great difference on NQWSE. Then the amplitude of NQWSE can be tuned adaptively and a better filtering effect can be achieved.

A more detailed form of equation (21) is

$$\mathbf{qwse} = \left(w_0^1 \times w_0^2 \times \cdots \times w_0^n\right)^2[0, 0, \ldots, 0]$$
$$+ \left(w_0^1 \times w_0^2 \times \cdots \times w_1^n\right)^2[0, 0, \ldots, r_n] + \cdots \quad (22)$$
$$+ \left(w_1^1 \times w_1^2 \times \cdots \times w_1^n\right)^2[r_1, r_2, \ldots, r_n].$$

5.2. Property Analysis of NQWSE. It is known by analyzing equation (22) that the NQWSE is the compound of all the QMSEs which are entirely contained in the quantum system. The quantum-inspired weightings of different QMSEs are determined by using stochastic information of the signal itself. Regarding $\mathbf{rs}(k)$ as the analyzing signal and integrating the formation process of quantum-inspired weighting and SE amplitude, it is possible to show that NQWSE has the following properties:

(1) In $|\mathbf{i}_b\rangle$, the bit $|\mathbf{i}_b\rangle(j)$ related to impulse response signal has a larger probability to obtain $|1\rangle$. After mapping to real space, the bit $\mathbf{g}(j)$ related to impulse response signal has a larger probability to obtain

QMSE amplitude $\mathbf{r}_j$. Therefore, QMSE amplitude $\mathbf{r}_j$ has a larger quantum-inspired weighting in NQWSE, and it is more possible to highlight the failure information after operating erosion.

(2) In $|\mathbf{i}_b\rangle$, the bit $|\mathbf{i}_b\rangle\,(j)$ not related to impulse response signal has a larger probability to obtain $|0\rangle$. After mapping to real space, the bit $\mathbf{g}(j)$ related to impulse response signal has a larger probability to obtain 0. Therefore, QMSE amplitude $\mathbf{r}_j$ has a smaller quantum-inspired weighting in NQWSE, and it is less possible to highlight the normal information after operating erosion.

(3) Only the QMSE amplitude $\mathbf{r}_j$ can affect the amplitude of NQWSE. That is to say, in nature, the amplitude of NQWSE is totally determined by QMSE amplitude $\mathbf{r}_j$ and quantum-inspired weighting W_i^2 of corresponding QMSE.

(4) At different sampling point, NQWSE is always different. The amplitude of NQWSE adjusts dynamically as the signal varies.

5.3. Procedure for the Algorithm. The specific procedure of applying NQWSE to MMF to process bearing impulse response signal is stated as follow:

Step 1. sample a bearing failure signal and the sampling signal $\mathbf{s}(k)$ is acquired

Step 2. invert $\mathbf{s}(k)$ to $\mathbf{rs}(k)$ according to equation (2)

Step 3. form the NQWSE according to Figure 2

Step 4. apply the NQWSE to $\mathbf{rs}(k)$ for erosion and the $\mathbf{re}(k)$ is acquired

Step 5. invert $\mathbf{re}(k)$ and the final signal is acquired.

Because the original sampling is inverted in Step 2, the signal is inverted again in Step 5 after MMF processing for the ease of observing.

6. Application Analysis

The bearing vibration signal used in this paper was acquired from a mechanical power-shift steering transmission. The schematic illustration of the mechanical transmission experimental system is shown in Figure 3. The test apparatus consists of a reliance electric motor, an accelerometer transducer located on tank cover over the faulted bearing, and a data recorder with a sampling frequency of 10,000 Hz per channel. The transducer is manufactured by Dytran with product model 3256A3T. The single point fault was introduced to the rolling element bearing at the inner raceway using electrodischarge machining with a fault diameter of 3 mm and fault depth of 2 mm. The shaft rotational speed was 1830 rpm (30.5 Hz). The sampling time was 0.6 second. On the basis of the theoretical calculation, the characteristic frequency of inner race fault is 158 Hz. The waveform of the
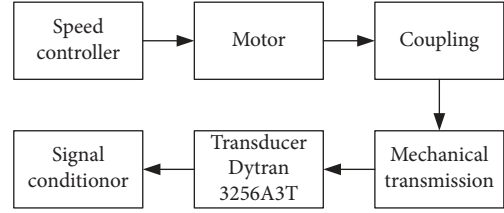

Figure 3: The schematic illustration of the mechanical transmission experimental system.

analyzed signal in the time domain and the envelop frequency spectrum are displayed in Figure 4. The defect frequency 158 Hz and its harmonics are blurred by other frequencies carrying unuseful information (Figure 4(b)), which leads to difficulty in detecting the fault.

Use NQWSE and CSE to operate erosion, respectively. The MMF filtering results is shown in Figures 5 and 6, respectively.

At the same time, the closing operator of CSE is performed for it has a greater ability of extracting failure information than that of erosion, and the results is shown in Figure 7. The CSE is set to the best size of 46 referring to reference [25], and its amplitude is set to 0.

6.1. Waveform. The three approaches can extract impulsive shapes in the time domain. The CSE leads to waveform distortion shown in Figures 6(a) and 7(a). However, the erosion results of NQWSE are preferable because they preserve the details of the signal.

6.2. Spectrum. Since the fault frequency is modulated by rotating frequency, the failure spectrum of bearing inner race fault has two typical characteristics: (1) there are rotating frequency and its harmonics in the spectrum and (2) there exist subbands around the fault frequency and its harmonics. And the difference between the subbands and its center frequency equals rotating frequency. Observing the spectrum of the three approaches, only the approach employing NQWSE to erosion can accord well with the above two characteristics, which indicates that the NQWSE has a better capability to extract impulse response signal.

6.3. Quantitative Comparison. For objective assessment of the extraction ability to impulse response signal, the characteristics intensity coefficient is employed for quantitative comparison. The characteristics intensity coefficient is defined as [8]

$$C_f = \frac{\sum_{i=1}^{N} \mathbf{FC}_i}{\sum_{j=1}^{M} \mathbf{F}_j}, \tag{23}$$

where $\mathbf{F}_j$ denotes the magnitude of each frequency and $\mathbf{FC}_j$ denotes the magnitude of each fault characteristics frequency. In this paper, let $N = 2$.

C_f indicates the energy proportion that the characteristics frequency possesses. The larger the C_f is, the more
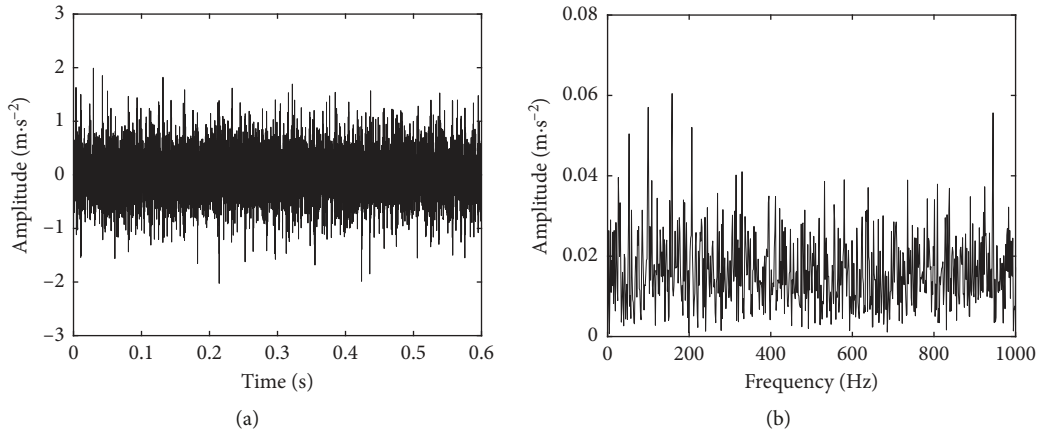
FIGURE 4: Fault signal with strong noise. (a) Waveform in the time domain. (b) Envelope frequency spectrum.
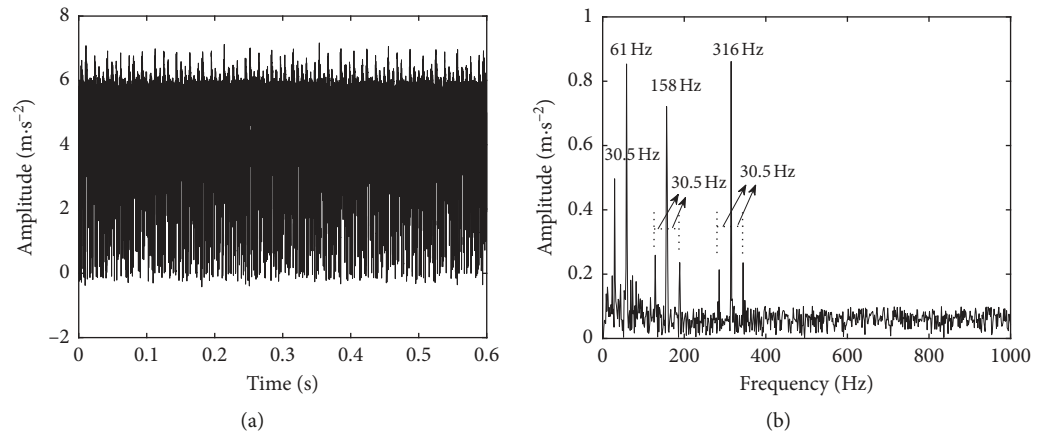

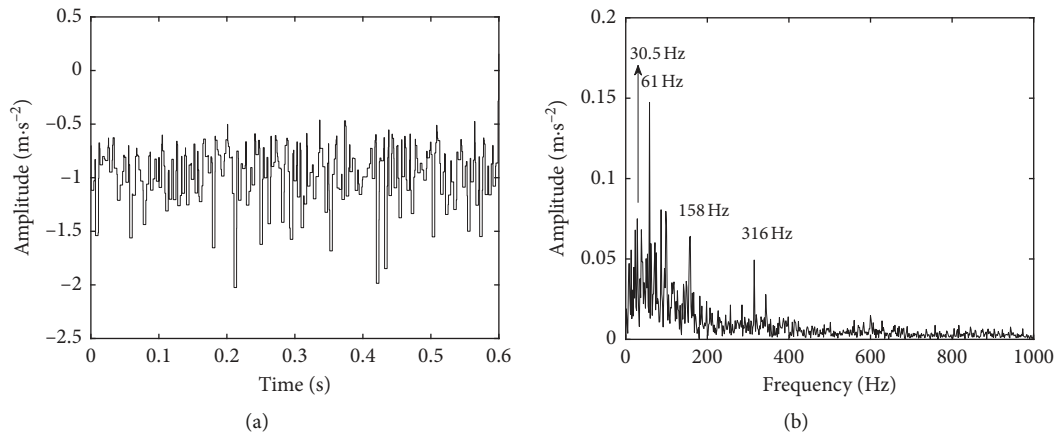FIGURE 5: Erosion results of NQWSE. (a) Waveform in the time domain. (b) Frequency spectrum.

FIGURE 6: Erosion results of CSE. (a) Waveform in the time domain. (b) Frequency spectrum.

easily the characteristics and its harmonics are observed. Table 1 lists the C_f computed by using NQWSE and CSE. The values show that NQWSE has the best result.

Figure 8 shows the results from the wavelet thresholding technique. The fault frequency located at 158 Hz can be clearly

identified, and the waveform indicates that a part of impulsive signal is extracted. However, the spectrum is still buried by other frequency components, which results in difficulty of detecting fault. Harmonic frequency values of characteristic frequency are too small to be used for failure recognition.
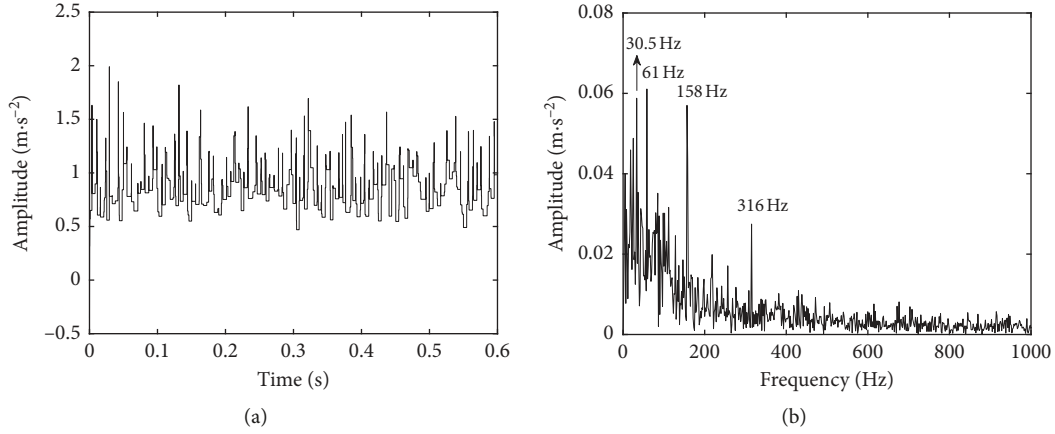
FIGURE 7: Closing results of CSE. (a) Waveform in the time domain. (b) Frequency spectrum.

TABLE 1: Comparison of C_f.

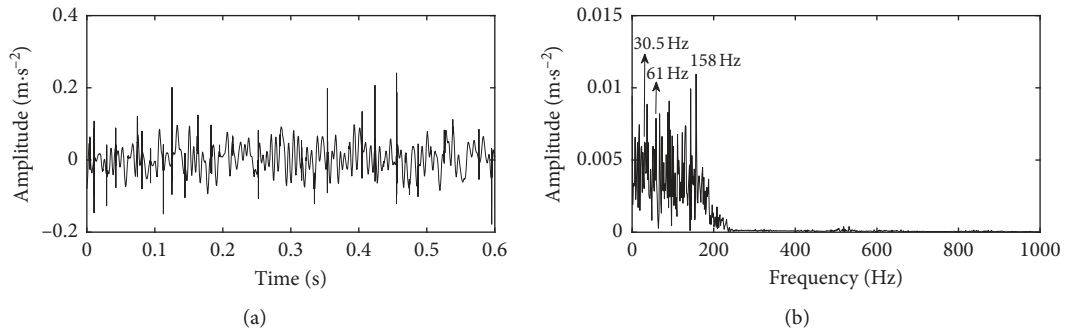| Approach	SE	C_f
Erosion	NQWSE	0.0082
Erosion	CSE	0.0033
Closing	CSE	0.0052

FIGURE 8: Results of wavelet thresholding. (a) Waveform in the time domain. (b) Frequency spectrum.

From the above, the NQWSE gives the most satisfactory results for signal: the noise is depressed and the fault information is extracted exactly.

7. Conclusions

In this work, we develop NQWSE, a new structuring element based on the erosion operator, combining the quantum theory with the local feature and stochastic characteristics of the signal. NQWSE adjusts its amplitude adaptively according to signal changes, and it can be used to extract the failure information which is represented as an impulse response signal. The experimental results show that the NQWSE has better extraction capacity for impulse response signal with respect to mere conventional techniques. The NQWSE has two advantages compared with CSE. (1) The amplitude of the NQWSE adjusts its amplitude according to local feature of signal, which leads to greater adaptively. Therefore, the NQWSE can analyze the different shapes of the signal while

the CSE can only extract specific shape. (2) The quantum-inspired weighting is generated via stochastic characteristics of signal, which guarantee the extraction capacity of NQWSE for impulse response signal and solve the disadvantage that the CSE is limited while applied to nonstable and nonlinear signals. However, the CSE used to generate NQWSE is based on the simplest SE [0, 0, 0, . . ., 0]. In the future, we will try to investigate other types of SEs and to analyze their properties for a more effective signal processing.

Data Availability

The data used to support the findings of this study are available from the corresponding author upon request.

Conflicts of Interest

The authors declare that there are no conflicts of interest regarding the publication of this paper.

Acknowledgments

References

[1] P. H. Rodríguez, J. B. Alonso, M. A. Ferrer, and C. M. Travieso, "Application of the Teager–Kaiser energy operator in bearing fault diagnosis," *ISA Transactions*, vol. 52, no. 2, pp. 278–284, 2013.

[2] Y. Zhang, H. Zuo, and F. Bai, "Classification of fault location and performance degradation of a roller bearing," *Measurement*, vol. 46, no. 3, pp. 1178–1189, 2013.

[3] D. H. Pandya, S. H. Upadhyay, and S. P. Harsha, "Fault diagnosis of rolling element bearing with intrinsic mode function of acoustic emission data using APF-KNN," *Expert Systems with Applications*, vol. 40, no. 10, pp. 4137–4145, 2013.

[4] Y. Imaouchen, M. Kedadouche, R. Alkama, and M. Thomas, "A Frequency-Weighted Energy Operator and complementary ensemble empirical mode decomposition for bearing fault detection," *Mechanical Systems and Signal Processing*, vol. 82, pp. 103–116, 2017.

[5] S. Wan and X. Zhang, "Teager energy entropy ratio of wavelet packet transform and its application in bearing fault diagnosis," *Entropy*, vol. 20, no. 5, p. 388, 2018.

[6] Y. Lei, J. Lin, Z. He, and M. J. Zuo, "A review on empirical mode decomposition in fault diagnosis of rotating machinery," *Mechanical Systems and Signal Processing*, vol. 35, no. 1-2, pp. 108–126, 2013.

[7] R. Yan, R. X. Gao, and X. Chen, "Wavelets for fault diagnosis of rotary machines: a review with applications," *Signal Processing*, vol. 96, pp. 1–15, 2014.

[8] B. Li, P.-L. Zhang, Z.-J. Wang, S.-S. Mi, and Y.-T. Zhang, "Gear fault detection using multi-scale morphological filters," *Measurement*, vol. 44, no. 10, pp. 2078–2089, 2011.

[9] H. Li and D.-Y. Xiao, "Fault diagnosis using pattern classification based on one-dimensional adaptive rank-order morphological filter," *Journal of Process Control*, vol. 22, no. 2, pp. 436–449, 2012.

[10] B. Li, P.-L. Zhang, Z.-J. Wang, S.-S. Mi, and D.-S. Liu, "A weighted multi-scale morphological gradient filter for rolling element bearing fault detection," *ISA Transactions*, vol. 50, no. 4, pp. 599–608, 2011.

[11] A. Layeb, "A hybrid quantum inspired harmony search algorithm for 0-1 optimization problems," *Journal of Computational and Applied Mathematics*, vol. 253, pp. 14–25, 2013.

[12] M. Soleimanpour-moghadam, H. Nezamabadi-pour, and M. M. Farsangi, "A quantum inspired gravitational search algorithm for numerical function optimization," *Information Sciences*, vol. 267, pp. 83–100, 2013.

[13] P. Li, "A quantum-behaved evolutionary algorithm based on the Bloch spherical search," *Communications in Nonlinear Science and Numerical Simulation*, vol. 19, no. 4, pp. 763–771, 2014.

[14] T.-C. Lu, G.-R. Yu, and G.-R. Yu, "An adaptive population multi-objective quantum-inspired evolutionary algorithm for multi-objective 0/1 knapsack problems," *Information Sciences*, vol. 243, pp. 39–56, 2013.

[15] G. Zhao, S. Zhao, Z. Yao et al., "Forward spectral filtering parallel quantum key distribution system," *Optics Communications*, vol. 298-299, pp. 254–259, 2013.

[16] J. S. Shaari and A. A. Bahari, "Improved two-way six-state protocol for quantum key distribution," *Physics Letters A*, vol. 376, no. 45, pp. 2962–2966, 2012.

[17] A. Akhshani, A. Akhavan, S.-C. Lim, and Z. Hassan, "An image encryption scheme based on quantum logistic map," *Communications in Nonlinear Science and Numerical Simulation*, vol. 17, no. 12, pp. 4653–4661, 2012.

[18] Y. Li, S. Feng, X. Zhang, and L. Jiao, "SAR image segmentation based on quantum-inspired multiobjective evolutionary clustering algorithm," *Information Processing Letters*, vol. 114, no. 6, pp. 287–293, 2014.

[19] J. Tsa, F. Y. Hsiao, Y. J. Li, and J. F. Shen, "A quantum search algorithm for future spacecraft attitude determination," *Acta Astronautica*, vol. 68, no. 7-8, pp. 1208–1218, 2011.

[20] Q. Niu, T. Zhou, M. Fei, and B. Wang, "An efficient quantum immune algorithm to minimize mean flow time for hybrid flow shop problems," *Mathematics and Computers in Simulation*, vol. 84, pp. 1–25, 2012.

[21] Y. Chen, P. Zhang, Z. Wang, W. Yang, and Y. Yang, "Denoising algorithm for mechanical vibration signal using quantum Hadamard transformation," *Measurement*, vol. 66, pp. 168–175, 2015.

[22] S. Yuan, X. Mao, L. Chen, and Y. Xue, "Quantum digital image processing algorithms based on quantum measurement," *Optik*, vol. 124, no. 23, pp. 6386–6390, 2013.

[23] X. W. Fu, M. Y. Ding, and C. Cai, "Despeckling of medical ultrasound images based on quantum-inspired adaptive threshold," *Electronics letters*, vol. 46, no. 13, pp. 21-22, 2010.

[24] P. L. Zhang, Y. L. Chen, H. G. Wang, and S. Li, "Compound quantum—inspired structuring element considering signal characteristics," *Journal of Jilin University(Engineering and Technology Edition)*, vol. 45, no. 4, pp. 1181–1188, 2015.

[25] N. G. Nikolaou and I. A. Antoniadis, "Application of morphological operators as envelope extractors for impulsive-type periodic signals," *Mechanical Systems and Signal Processing*, vol. 17, no. 6, pp. 1147–1162, 2003.